Influence of laser scanning power on microstructure and tribological behavior of NI-composite claddings fabricated on TC4 titanium alloy

Md. Helal Miah
Department of Mechanical Engineering, Chandigarh University, Mohali, India
Dharmahinder Singh Chand and Gurmail Singh Malhi
Department of Aerospace Engineering, Chandigarh University, Mohali, India, and
Shahrukh Khan
Department of Aircraft Maintenance Engineering, Bangabandhu Sheikh Mujibur Rahman Aviation and Aerospace University, Dhaka, Bangladesh

Abstract

Purpose – The demand for titanium alloys has received massive attention in the aerospace and automotive industry owing to their magnificent electrochemically compatibility and corrosion resistance, high strength at elevated temperatures and high strength-to-weight ratio. Although titanium alloy has impressive mechanical properties, they are challenging to machine or metal form due to its poor heat conductivity, high chemical reactivity, low modulus of elasticity, high friction coefficient and difficult lubricant that limits its application field and increases wear. However, surface treatment coating with the strong metallurgical bond between the titanium alloy matrixes is novel technique to resolve these challenges. This research will illustrate the influence of laser scanning power on the microstructure and tribological behavior of Nickel (NI)-composite claddings fabricated on TC4 titanium alloy to realize the strong metallurgical bond between the titanium alloy and NI-composite coating.

Design/methodology/approach – In this research, TiC/TC4 alloy nanocomposites were fabricated based on different laser power and temperatures. TC4 has been selected as a base material instead of TiC for the strong metallurgical bond between the titanium alloy matrixes. Then Ni-composite coating was used as the surface treatment coating on TC4 by laser cladding (LC) technique. The Ni-based alloy coating material powder is good self-fluxing, has high-temperature resistance and is analytically pure with 200 mesh, which can easily overcome the various challenges of titanium alloy. The chemical properties of Ni composite coating include 31.2% Chromium, 8%Titenium and 3.6% Carbon. The prepared surface treatment coating characterization and microstructure behavior are analyzed using optical micrograph, X-ray diffraction, scanning electron microscopes, energy dispersive spectroscopy and electron probe micro analyzer methods.

Findings – It is evident that at the beginning of the experiment, if the laser power increased, the quality of the coating increased. An optimal quality of the coating is found when the laser scanning power about 12.55 kJ/cm^2. Further increased laser power diminished the quality of the coating because the material plasticity had deteriorated. The TiC ceramic particle reinforced phase is dispersed into a two-phase solid solution of β-Ti and γ-Ni. The micro-hardness of the used coating is greater than the base alloy.

Originality/value – This research has practical value in the modern aerospace and automobile industry to increase the application of titanium alloy.

Keywords Titanium alloy, Laser cladding, Surface treatment coating, Microstructure analysis, Mechanical analysis

Paper type Research paper

1. Introduction

Surface engineering involves adding material or changing surface topography, which is a novel technique for tribological solutions in chemical, structural and morphological alteration for the surfaces of any object. The application of surface engineering can increase hardness and wear resistance, decrease friction and wear and improve mechanical performance. Any mechanical engineering field component's surface is a crucial component. It is common knowledge that surface-initiated flaws, such as wear, corrosion, fatigue or fracture, are the leading causes of component failure. Surfaces with increased tribological performance have worldwide demand, especially in the aircraft industry (Sultana *et al.*, 2021). Contrary to bulk alloying, surface engineering offers the chance to increase the wear resistance of

The current issue and full text archive of this journal is available on Emerald Insight at: **https://www.emerald.com/insight/1748-8842.htm**

Aircraft Engineering and Aerospace Technology
95/8 (2023) 1165–1171
 [ISSN 1748-8842]
[DOI 10.1108/AEAT-06-2022-0145]

Received 4 June 2022
Revised 30 November 2022
16 February 2023
Accepted 20 March 2023

engineering materials while mostly maintaining the bulk properties. The current study aims to enhance the wear of titanium-based alloys by texturizing and coating their surfaces. It will be functionally equivalent to titanium alloy used in automotive and structural applications (Vasudev *et al.*, 2019).

Surface texturing modifies the surface's topography, producing a similar micro-relief with typical asperities or dimples as this innovative process significantly increases the surface contact area between the coating and substrate, concerning the surface being changed physically and mechanically. In addition, it enhances the tribological qualities of substrate materials and coating adherence. The most cutting-edge and newly developed texturing technique is laser surface texturing. This method uses a material ablation procedure with a pulsing laser beam to create synthetic, regularly designed micro dimples on the substrate surface. The quality of the surface that will later be covered by physical vapor deposition depends on the laser and scanner settings, which also affect the precision of texturing. To minimize the use of lubricant, surface texturing offers micro-reservoirs or micro-traps to hold on to wear debris (Ananth and Ramesh, 2017).

The alloys of titanium have massive potential in aerospace, aviation, petroleum and chemical industries as structural materials owing to their high allowable strength, exceptional corrosion resistance, excellent oxidation resistance and less thermal expansion coefficient (Williams and Boyer, 2020). It can be fabricated by the surface of titanium alloy with good wear resistance and oxidation resistance using advanced surface modification technology (Zhang *et al.*, 2020). However, the friction coefficient of titanium alloys is not suitable for plastic forming and machining due to high friction, severe adhesive wear and difficulty to lubricate, which limits its application range (Khanna and Sangwan, 2013). To tackle these challenges, surface modification with coating, which forms a strong metallurgical bond between the matrixes of titanium alloy can be the possible solution (Reddy *et al.*, 2013). TiC/TC4 has excellent hardness value, high wear resistance, minimal friction coefficient and outstanding hardness and chemical stability. That is why it can be considered as an excellent coating material (Wang *et al.*, 2008). The alloy/ceramic composite coating method can obtain good coating performance. Researcher at home and abroad have used ample amount of research on alloy/ceramic composite coating method (Liu *et al.*, 2014).

- Gadow and Scherer (2002) examined composite coatings with dry lubrication capabilities on light metal substrates. In the absence of lubrication, light metals have inferior tribological characteristics that cause severe seizing and wear. They assessed the composite coatings made of a secondary chemical vapor deposition (CVD)/physical vapor deposition (PVD)-deposited layer and a primary ceramic (TiO_2) layer that was thermally sprayed (polytetrafluoroethylene and MoS_2). The primary coating, which is thermally sprayed, offers compressive strength, hardness and wear resistance, protecting the light metal substrate. The secondary layer causes low friction (Gadow and Scherer, 2002).
- Sousa *et al.* (2021) investigated the high-speed cutting capabilities of a TiAlN coating using interlayers that have low elastic moduli, such as Ti, Cu and Al. All coatings have columnar microstructures, and the coating hardness is different interlayer to interlayer. Ti and Al interlayers increased the coating's elastic modulus, but the Cu interlayer caused a drop. Because of its high ductility, the copper interlayer lowers the adhesion and residual compressive stresses of the TiAlN coating compared to the Ti and Al interlayers. Chemical affinity is a key aspect in improving coating performance; the coating structure of the interlayer has no influence on coating performance (Sousa *et al.*, 2021).
- Shum *et al.* (2007) explored that the carbon ion implantation pretreatment improved the bonding strength of the pure carbon coating on the Ti6Al4V substrate. The coatings created on substrates with carbon implants considerably enhanced bonding strength, wear resistance and impact resistance. The enhanced hardness and solid Ti–C bonding by the ion implantation contributed to the coating's better performance (Shum *et al.*, 2007).
- The effect of metallic interlayers on the adhesion of TiN coatings on high-speed steel was investigated by Gerth and Wiklund (2008). According to the scratch test results, adhesion between the metallic interlayers had a greater influence on hardness differences than elastic modulus differences. The thermal coefficient of expansion of the interlayer should be close to the top layer coating and substrate material for improved adhesion (Gerth and Wiklund, 2008).
- Three different hydrogenated amorphous carbon (a-C: H) coatings on Ti6Al4V substrate were studied by Martini *et al.* (2011). Amorphous carbon coating was done using the plasma assisted (PA)-CVD technique, whereas CrN interlayer deposition was done using the PVD technique. A slider on the cylinder tribometer was used to examine the friction and wear behavior of the coated samples against the 100Cr6 counter body. The high penetration coating of a-CH was less thick and less adhering than the conventional coating but exceedingly rigid and stiff. This results in little friction and wear at low normal loads but fails quickly at high normal loads. Due to its improved load support, the CrN interlayer increases the a-C: H coating's adhesion to the substrate and has higher wear resistance under all typical loads (Martini *et al.*, 2011).

However, most studies are limited to analysis of coating structure and performance (coating hardness, wear resistance, etc.) and the influence of laser process parameters on coating quality (Weng *et al.*, 2014). There are few studies on the distribution of chemical components and the distribution in the microstructure. The chemical composition distribution in the coating directly determines its microstructure, and it is the most concerned coating in the production field (Sun *et al.*, 2001). The performance of the coating has a decisive influence (Ma and Matthews, 2009). Therefore, it is necessary to explore the influence of process parameters to maximize the coating quality and the excellent structure of the coating micro-area and the chemical composition distribution. In this experiment, a high-power laser is used to prepare the original surface of the TC4 in situ TiC particle-reinforced Nickel (Ni)-based composite coating. Characterization means like "Optical Micrograph" (OM), "X-Ray Diffraction" (XRD), "Scanning Electron Microscopes" (SEM), "Energy Dispersive Spectroscopy" (EDS) and "Electron Probe Micro

Analyzer" (EPMA) perform overall characterization and microstructure analysis of the prepared coating and analyze the structure of the cladding layer with different laser scanning power (LSP) performance impact.

2. Materials and method

The TC4 (Ti–6Al–4V) titanium alloy is selected as the base experimental material, and the sample size is 30 mm × 20mm × 10mm. The coating material is Ni-based alloy powder with good self-fluxing and high-temperature resistance, and chemical composition 31.2%Cr, 8%Ti, 3.6%C. Also, Ni-alloy is analytically pure with 200 mesh. The earlier mentioned powders are mixed by mechanical grinding, evenly coated on the substrate surface with a thickness of 0.6 mm after mixing with an organic binder, then dried using the DLHL-T50000B fast axial flow CO_2 exciter under the protection of Argon gas. In the laser cladding (LC) experiment, the following laser process parameters (as shown in Table 1) are used.

First, an XRD-6000 is used to analyze the phase composition of the composite coating surface. After grinding and polishing, a metallographic sample is prepared. The sample is cut along the cross-section of the coating. The MEF3 multifunctional metallographic microscope, JSM-5600LV SEM, accessories LINKISIS6587 energy dispersive spectrometer and EPMA-1600 electron probe instrument are used for coating cross-section microstructure characteristics analysis.

The micro-hardness values of the cladding layer were assessed using a micro Vickers hardness tester with a load of 200 g along the cross-section as this is the standard scale for hard coatings. From the surface to the bulk, the hardness was assessed along the nickel-composite cross section (*X*-axis) (along *Y*-axis). The average micro-hardness value was calculated using five separate measurements for each specimen, and the hardness profile along the melt direction is shown in the next section.

The XRD data were gathered for the 2θ spanning from 20° to 100° in steps of 1/min using the Philips 3121 X-ray diffractometer with γ-Ni and α-Ti radiation at 40 kV and 200 mA. Hank's solution was used to study the friction behavior of the LC samples at 37 ± 1°C for 10^5 cycles by monitoring the weight loss concerning the wear tests with an electronic balance (0.0001 g precision). Three friction coefficient graphs were created (sliding step versus friction coefficient) using the information gathered during the wear test.

3. Result and discussion

3.1 The quality of the laser cladding layer

Table 2. lists the LC process parameters (LSP= P/vD) and their influence on the quality of the cladding layer. When the LSP was low, defects (pores and cracks) appeared in the cladding layer and the surface appeared relatively rough. With increase in particular energy of the laser, the structure in the cladding layer turn out to be uniform and the surface is more smooth. With the LSP 12.5 kJ/cm^2, a defect-free coating was obtained. With further increase in LSP, the cladding cracks appeared in the coating layer again. Due to the extremely fast heating and cooling speed of LC, the lifecycle of the molten pool was very short, but the oxides and other impurities probably existed in the molten layer are often too late to release the source of pores and cracks. In addition, the cladding layer solidified and crystallized instantly, dislocations at grain boundaries, increased vacancies, extremely irregular atomic arrangement and increased solidification defects. At the same time, the thermal brittleness increased, the plastic toughness decreased and the cracking sensitivity increased. Generally speaking, increasing the existence time of the molten pool means increasing the LSP, which can reduce the occurrence of defects. However, a further increase in the LSP may cause the surface of the coating to be burned and oxidized, resulting in new defects.

Table 1 Laser process parameters

Output power (P)	Scanning speed	Spot diameter	Multi-channel overlap rate
2~6 kW	5~12 mm/s	2mm	30%

Table 2 The LC process parameters

Sample no	Laser specific energy/(kJ cm^{-2})	Cladding layer quality
S1	8.34	Pores and cracks
S2	10.00	A few pores and cracks
S3	12.50	Almost defect-free
S4	14.30	A few cracks
S5	16.70	Cracked

Figure 1 shows the structure of the S3 (almost defect-free) cladding layer of the sample with good cladding quality. The distribution seems in a regular orientation, basically consistent with the direction of heat flow. It also be observed from the structure that the overall cladding of the coating is good, and the thickness is appropriate. The dendrite structure in the melting zone inside the coating has been developed, which is good, uniform and smoother coating surface.

In Figure 1, A1 denotes the cross-section area of sample S3, and A2 denotes the melting zone of the S3. The cladding zone, bonding zone and heat-affected zone make up the macro morphology.

Figure 2 is the SEM morphology of the cross-section of the sample S3 composite coating. It may be revealed from the overall structure because there is probable formation of a bonding layer (II in Figure 2) between the cladding layer and the heat-affected zone, but there is no bonding interface between the layers.

The result of the energy spectrum composition analysis of each layered area in Figure 2 (Table 3) shows that the prime components between the substrate and the coating material have been diffused each other, which indicates that the substrate and the coating have achieved good results. It can be seen from the bonding interface of the cladding layer and the bonding layer in Figure 2 that the structure of the cladding layer and the bonding layer is got staggered. And some of the structures in the cladding layer are inserted into the matrix like a wedge. The structure ensures that the cladding layer got firmly bonded to the substrate and the bonding interface has sufficient strength. The structure of the cladding layer near the bonding layer is distributed in a gradient; it ensures the quality of the coating.

Figure 1 Microstructure of the cross-section of the sample S3 (a) microscopic morphology; (b) dendrite structure of coating

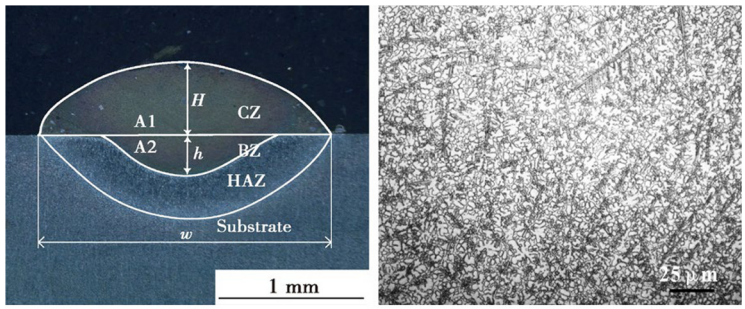

Figure 2 Cross-sectional SEM morphology of Sample 3

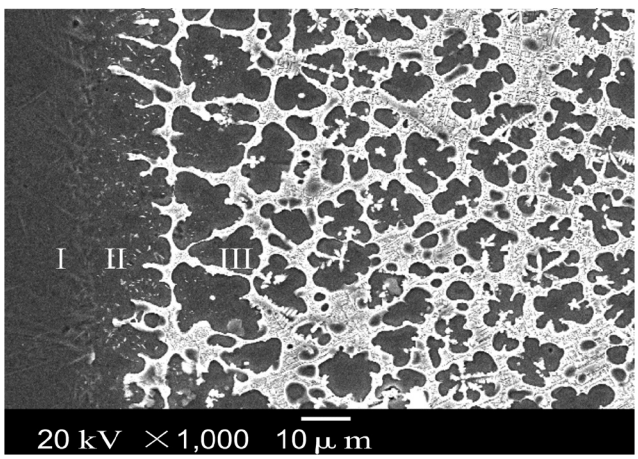

3.2 Coating structure and microhardness

Figure 3(a)–(c) are SEM pictures of the cladding layer structure of samples S1, S3 and S5. SEM shows the dendritic area is not corrosion resistant and presents pits; in addition, the interdendritic is corrosion resistant, with strong white petal particles and network structure.

The S1, S3 and S5 sample cladding area structure is distributed on the network dendritic and eutectic matrix with white cross-petal-shaped particles and white bright fine spherical particles. In S5, there is also a thin spike-like structure. The structure of the S3 sample is coarser and more regular than S1, and there are more white and bright spherical particles than S1 and S5. The phase composition of S3 (phase composition S1, S2, S3, S4 and S5 are same) are γ-Ni, TiC, $NiTi_2$, Ni_3C, M_7C_3, etc. (Figure 4). Combining EDS and EMPA can analyze the composition of each structure in the cladding zone as follows:

- The key phases of the dendrite is Ni, and the phase is γ-Ni, Ni_3C and $NiTi_2$, among which a large amount of Ti, Cr and other elements are dissolved in γ-Ni, which has excellent toughness and corrosion resistance.
- In the LC process, the cooling speed of the laser molten pool is extremely fast, and the high temperature makes the melt.
- The elements such as Ti and Cr in the Ni-based alloy melt are too late to precipitate during the rapid cooling process and are dissolved in the γ-Ni to form an extended solid solution. Therefore, it will inevitably cause a significant solid solution strengthening effect and increase the hardness of the coating.
- The main component of the eutectic matrix is Ti, and the phase is β-Ti. Because the Ti phase changes to β-Ti during the rapid laser heating process, it is too late to transform into α-Ti during rapid solidification and remains at room temperature. It is a metastable phase with excellent comprehensive properties excellent toughness. β-Ti appears between the dendritic structure and the interdendritic brittle ceramic phase, which improves the brittleness of the coating due to the formation of the ceramic phase.
- The phase of the white cruciform petal-like particles is TiC. With witnessing its growth shape, it is found that the dendrite arms of the dendrites grow symmetrically, which is closely related to the crystal structure of TiC.
- TiC crystals have a face-centric cubic structure, Ti and C Atoms have a centrosymmetric structure, which leads to the formation of symmetric cruciform petal-like structure when TiC nucleates.

Chen *et al.* confirmed that the cruciform petal-like structure is the preferential growth of TiC along the direction of close-packed atoms (111) (Weng *et al.*, 2014). As a result, the white and bright fine spherical particles are M_7C_3. The short rod-shaped structure

Table 3 Chemical properties of coating in different areas

Zone	Titanium- (Ti)	Aluminum- (Al)	*w*/% Vanadium- (V)	Nickel- (Ni)	Chromium- (Cr)	Carbon- (C)
Zone I	90.240	5.295	3.840	–	–	–
Zone II	64.165	2.730	1.580	25.365	5.365	0.815
Zone III	28.930	0.720	–	44.430	23.565	1.250

Figure 3 SEM morphology of the cladding zone for samples (a) S1; (b) S3 and (c) S5

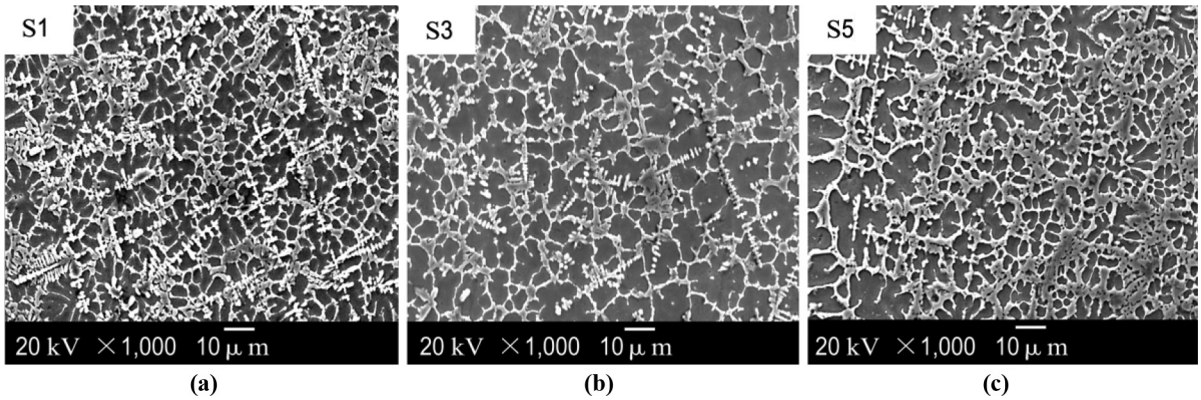

Figure 4 XRD analysis graph of sample S3 coating surface

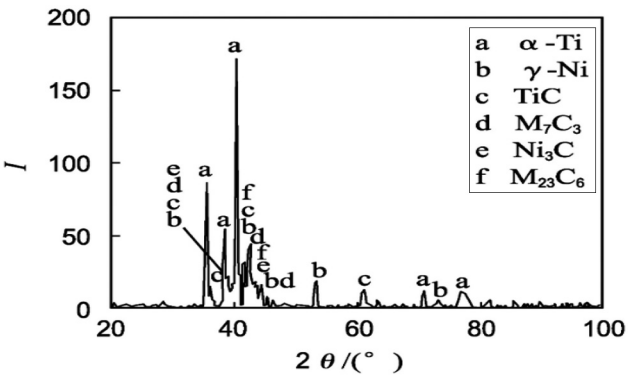

Figure 5 Microhardness graph of specimens S1, S3 and S5 cross-sections

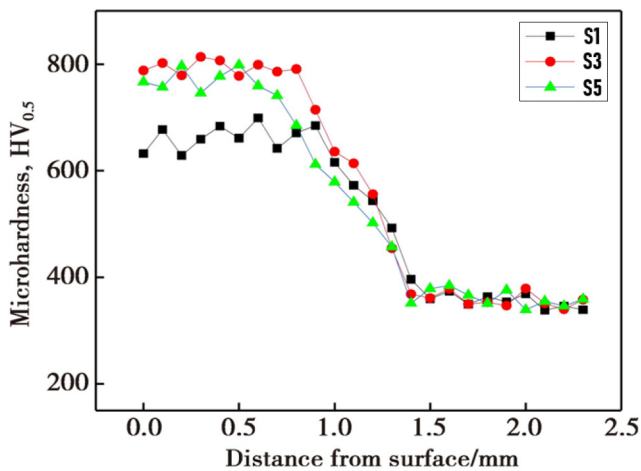

in the S5 sample is mainly composed of Cr, and the phase is $M_{23}C_6$, and part of the Cr is replaced by Ni and Ti. In the superalloy, when Cr is relatively higher than C, when the content is higher, the precipitation tendency of the $M_{23}C_6$ phase is relatively large, and the phase is distributed in a short rod shape at the grain boundary.

Figure 5 shows the optimized results of the microhardness of the samples S1, S3 and S5. The microhardness values of the different samples from the surface to the substrate show a gradient distribution in the depth direction of the cladding. The hardness of the LC layer (HV850–950) is compared with the base alloy (HV330–340). The change of the LSP has a significant effect on the hardness value. However, the particular energy of the laser is further increased, increasing the dilution rate of the coating and a decrease in the relative content of the reinforcing phase. When the LSP was 12.5 kJ/cm^2, the hardness found as highest one. The change of the microhardness value is closely related to the material's microstructure.

3.3 Analysis of coating micro-zone elements

Figure 6 is a typical S3 sample electron beam at low-speed scanning composite coating microscopic area EPMA composition analysis diagram. Figure 6 (a) and 6(b) is secondary electronic image and backscattered electron images in the coating, respectively. It can be seen that the morphological contrast and composition contrast in the molten zone are the same. It is evident that the formation of the morphology in the coating is closely related to the chemical composition distribution. Figure 6 (c)–(f) are, respectively, the surface distribution images of Ni, Ti, C and Cr in the same area. It can be seen from (c) that Ni is rich in dendrites, which is the γ-Ni solid solution. Ti, C presents a synchronous distribution in the micro-region, compared with (a) and (b). It can be observed that the distribution law of Ti and C is consistent with the morphological contrast and composition contrast in the micro-region. The C-enriched zone is the TiC phase in the inter-granular eutectic structure. It can be seen from (d) that there are good Ti-enriched particles in the area between the dendrites to the dendrite layer, and the content of C in the corresponding area is not high [Figure 6(e)]. This is due to the Ti phase transforming into β-Ti during the rapid laser heating process. It was too late to transform into α-Ti during rapid solidification and remained at room temperature. It can be seen from Figure 6(f) that Cr is evenly distributed between the dendrites, and the contents of Ni and Ti in the corresponding areas are higher. On the one hand, Cr forms a solid solution with Ni, and on the other hand, it forms M23C6. In conclusion, the XRD and SEM experimental results are accurately verified.

Figure 6 EPMA analysis diagram of micro-region of sample S3 composite coating (a) secondary image of S3; (b) black-scatter SEM image of S3; (c) Ni-surfaces SEM image of S3; (d) Ti-surfaces SEM image of S3; (e) C-surfaces SEM image of S3 and (f) Cr-surfaces SEM image of S3

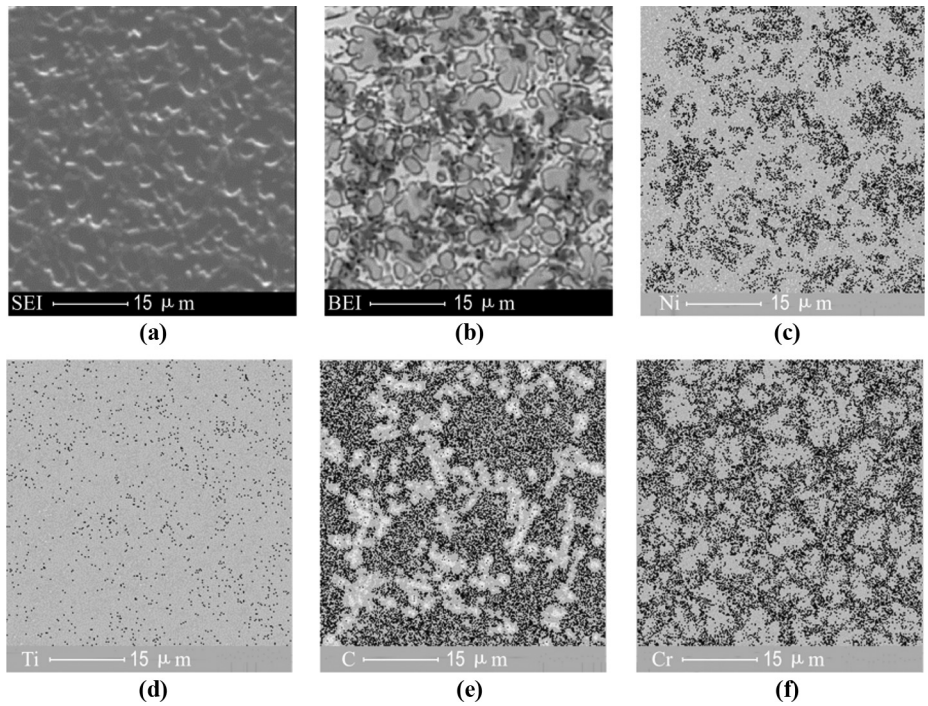

3.4 Friction coefficient and wear analysis

The comparison of the friction coefficient of samples S1, S2 and S3 with TC4 is shown in Figure 7. The maximum friction coefficient of the TC4 is around 0.63, and the fluctuation range is 0.03. As TC4 is selected as a based material for this experiment, it is evident that samples S1, S2 and S3 show less friction coefficient compared with the base material. The rank of the friction coefficient is TC4>S1>S3>S5. The friction coefficient is lowest when the LSP is 16.70 kJ/cm^2. The friction coefficient between the cladding layer and the substrate fluctuates within a narrower range (±0.01) for samples S1, S3 and S5. It is evident that the cladding layer has a higher degree of stability because the cladding layer generates challenging phases such as Ti_2Ni, TiB and TiC. During the friction and wear process, greater hardness can successfully inhibit the micro-cutting of abrasive particles. With the increase of the LSP, the cladding layer structure is a network structure with a large gap → a dense network structure →a dense bulk phase structure and a dense structure. The ability of the cladding layer to resist external particle cutting and plastic deformation can be improved, thereby reducing the friction coefficient of the cladding layer and improving the wear resistance of the cladding layer.

Figure 7 Comparison of the friction coefficient of coating sample S1, S2 and S3 with TC4 substrate

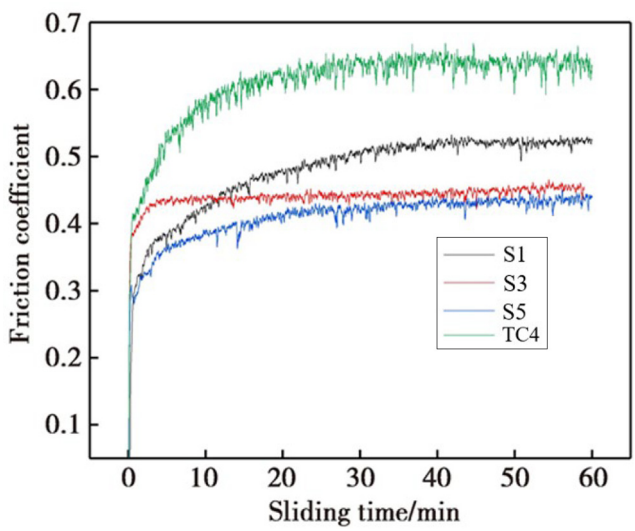

4. Conclusion

The primary reinforcement phase is a Ni-based cermet composite coating with a good combination of the matrix and TiC particles. It can be prepared on the surface of the TC4 alloy by optimizing laser process parameters using the preset NiCrTiC mixed powder method. The followings outcome is found in this research :

- With the increase of laser power, the coating equiaxed dendrites content and size increased simultaneously. The dendritic structure inside the composite coating comprises two phases of β-Ti and γ-Ni solid solution. The interdendritic is composed of TiC as the main hard ceramic phase is dispersed in the eutectic structure formed in the aforementioned solid solution.
- The hardness of the coating (HV850–950) is significantly higher than the base alloy (HV330–340). Among them, the hardness of the S3 (12.50 kJ/cm^2) sample was the best.

- A nickel interlayer's presence significantly influences the coating's ornamentation rate. The nickel interlayer had a lower wear rate than TC4. The optimal LSP (12.50 kJ/cm^2) considerably improved the coating's wear resistance.

References

Ananth, M.P. and Ramesh, R. (2017), "Sliding wear characteristics of solid lubricant coating on titanium alloy surface modified by laser texturing and ternary hard coatings", *Transactions of Nonferrous Metals Society of China*, Vol. 27 No. 4, pp. 839-847.

Gadow, R. and Scherer, D. (2002), "Composite coatings with dry lubrication ability on light metal substrates", *Surface and Coatings Technology*, Vols 151/152, pp. 471-477.

Gerth, J. and Wiklund, U. (2008), "The influence of metallic interlayers on the adhesion of PVD TiN coatings on high-speed steel", *Wear*, Vol. 264 Nos 9/10, pp. 885-892.

Khanna, N. and Sangwan, K.S. (2013), "Machinability study of α/β and β titanium alloys in different heat treatment conditions", *Proceedings of the Institution of Mechanical Engineers, Part B: Journal of Engineering Manufacture*, Vol. 227 No. 3, pp. 357-361, doi: 10.1177/0954405412469509.

Liu, X.B., Meng, X.J., Liu, H.Q., Shi, G.L., Wu, S.H., Sun, C. F., Wang, M.D. and Qi, L.H. (2014), "Development and characterization of laser clad high temperature self-lubricating wear resistant composite coatings on Ti–6Al–4V alloy", *Materials & Design, Elsevier*, Vol. 55, pp. 404-409.

Ma, X. and Matthews, A. (2009), "Evaluation of abradable seal coating mechanical properties", *Wear, Elsevier*, Vol. 267 Nos 9/10, pp. 1501-1510.

Martini, C., Ceschini, L., Casadei, B., Boromei, I. and Guion, J.B. (2011), "Dry sliding behaviour of hydrogenated amorphous carbon (aC: H) coatings on Ti-6Al-4V", *Wear*, Vol. 271 Nos 9/10, pp. 2025-2036.

Reddy, G.M., Rao, A.S. and Rao, K.S. (2013), "Friction stir surfacing route: effective strategy for the enhancement of wear resistance of Titanium alloy", *Transactions of the Indian Institute of Metals 2013*, Vol. 66 No. 3, pp. 231-238.

Shum, P.W., Zhou, Z.F. and Li, K.Y. (2007), "Enhancement of adhesion strength and tribological performance of pure carbon coatings on Ti-6Al-4V biomaterials with ion implantation pretreatments", *Tribology International*, Vol. 40 No. 2, pp. 313-318.

Sousa, V.F., Da Silva, F.J.G., Pinto, G.F., Baptista, A. and Alexandre, R. (2021), "Characteristics and wear mechanisms of TiAlN-based coatings for machining applications: a comprehensive review", *Metals*, Vol. 11 No. 2, p. 260.

Sultana, A., Zare, M., Luo, H. and Ramakrishna, S. (2021), "Surface engineering strategies to enhance the in situ performance of medical devices including atomic scale engineering", *International Journal of Molecular Sciences*, Vol. 22 No. 21, p. 11788.

Sun, L., Berndt, C.C., Gross, K.A. and Kucuk, A. (2001), "Material fundamentals and clinical performance of plasma-sprayed hydroxyapatite coatings: a review", *Journal of Biomedical Materials Research*, Vol. 58 No. 5, pp. 570-592.

Vasudev, H., Singh, G., Bansal, A., Vardhan, S. and Thakur, L. (2019), "Microwave heating and its applications in surface engineering: a review", *Materials Research Express*, Vol. 6 No. 10, p. 102001.

Wang, X.H., Zhang, M., Liu, X.M., Qu, S.Y. and Zou, Z.D. (2008), "Microstructure and wear properties of TiC/FeCrBSi surface composite coating prepared by laser cladding", *Surface and Coatings Technology, Elsevier*, Vol. 202 No. 15, pp. 3600-3606.

Weng, F., Chen, C. and Yu, H. (2014), "Research status of laser cladding on titanium and its alloys: a review", *Materials & Design*, Elsevier, Vol. 58, pp. 412-425.

Williams, J.C. and Boyer, R.R. (2020), "Opportunities and issues in the application of titanium alloys for aerospace components", *Metals 2020*, Vol. 10 No. 6, p. 705.

Zhang, L.C., Chen, L.Y. and Wang, L. (2020), "Surface modification of titanium and titanium alloys: technologies, developments, and future interests", *Advanced Engineering Materials*, Vol. 22 No. 5, p. 1901258.

Further reading

Al-Sayed Ali, S.R., Hussein, A.H.A., Nofal, A., Hassab Elnaby, S.I. and Elgazzar, H. (2019), "A contribution to laser cladding of Ti-6Al-4V titanium alloy", *Metallurgical Research & Technology*, Vol. 116 No. 6, p. 634.

Liu, F., Mao, Y., Lin, X., Zhou, B. and Qian, T. (2016), "Microstructure and high temperature oxidation resistance of Ti-Ni gradient coating on TA2 titanium alloy fabricated by laser cladding", *Optics & Laser Technology, Elsevier*, Vol. 83, pp. 140-147.

Wang, K., Du, D., Liu, G., Chang, B. and Hong, Y. (2019), "Microstructure and properties of WC reinforced Ni-based composite coatings with Y2O3 addition on titanium alloy by laser cladding", *Science and Technology of Welding and Joining*, Vol. 24 No. 5, pp. 517-524, doi: 10.1080/13621718.2019.1580441.

Corresponding author

Md. Helal Miah can be contacted at: helal.sau.12030704@gmail.com